The 2016 World Congress on
The 2016 Structures Congress (Structures16)
Jeju Island, Korea, August 28-September 1, 2016

URANS Computations of Cavitating Flow around a 2-D Wedge by Compressible Two-Phase Flow Solver

*Yohan Choe[1)], Hyeongjun Kim[1)], Chongam Kim[2)]

[1), 2)] *Department of Aerospace Engineering, Seoul National University, Seoul, Korea*
[2)] *Institute of Advanced Aerospace Technology, Seoul National University, Seoul, Korea*

ABSTRACT

This paper deals with the computation of unsteady cavitating flow around a two-dimensional wedge by using Unsteady Reynolds Averaged Navier-Stokes (URANS) flow solver. Because of accuracy deterioration problem due to excessive numerical dissipations for low Mach number unsteady flow, properly scaled RoeM and AUSMPW+ numerical flux schemes are used to accurately compute unsteady cavitating flow. Fast Fourier Transform (FFT) analysis results of experiments and computations are compared to show similar dominant frequencies of shedding vortices. Shedding pattern and location of vortices are also compared to show similar behavior of each flow result.

1. INTRODUCTION

A primary problem of two-phase flow is strongly-coupled acoustic phenomena because the speed of sound in two-phase mixture flow can be extremely low, compared with that in the individual component phases. For this reason, two-phase flow frequently undergoes an all-speed regime in which the flow may be transonic or even supersonic, although the bulk of the flow may remain essentially incompressible. In the computation of two-phase flow, therefore, system preconditioning is a major issue because of disparity of system eigenvalues. Preconditioning schemes that improve accuracy and convergence have proven to be highly successful for steady low Mach number flows [1, 2, 3]. However, these schemes have problems with both efficiency and accuracy for unsteady computation of low Mach number flow. For this reason, accurate and efficient computation of unsteady low Mach number flows has been an important issue. In order to achieve this, it is important to design numerical schemes for unsteady low Mach number flows that can provide computational efficiency over a broad range of flow conditions and compute flow physics accurately. Regarding the unsteady preconditioning, Venkateswaran et al. [4] found that Strouhal

[1)] Graduate Student(Ph. D. Candidate)
[2)] Professor, mail: [2)] chongam@snu.ac.kr

number should be considered in preconditioning process for convergence acceleration of unsteady low Mach number flows, and showed that optimal scaling is required for spatial accuracy.

As a previous work, we developed two-phase shock-stable numerical schemes [5] that originate from the RoeM [6] and AUSMPW+ [7] schemes. We showed that these extended numerical flux schemes are robust and efficient for compressible two-phase flow and that they can deal with compressible-incompressible two-phase flow through the application of steady preconditioning techniques. They are not able to compute unsteady low Mach number flow accurately because they do not take into account unsteady preconditioning and scaling of numerical flux schemes.

The purpose of this paper is to compute unsteady cavitating flow around a 2-D wedge by using compressible two-phase URANS solver. For the computation of unsteady low Mach number flow, we extend the previous all-speed two-phase RoeM and AUSMPW+ numerical flux schemes to the application of unsteady system preconditioning. We also scale numerical dissipations of the numerical flux schemes separately from the system preconditioning.

2. NUMERICAL METHODS

2.1 Governing equation

The homogeneous mixture equation with mass fraction is adopted as the governing equation for unsteady cavitating flow. In homogeneous flow theory, the relative motion between phases is not considered; instead, mixture is treated as a pseudo-fluid whose properties are suitable averages of each component in the flow. This approach is based on the view that it is sufficient to describe each phase as a continuum obtained from a microscopic description using a suitable averaging process. In this model, continuity, momentum, and energy equations are used to describe the fluid mixture, while a single continuity equation is used for vapor and non-condensable gas phases. The governing equation is as follows,

$$\frac{\partial}{\partial t}\int_{\Omega} W\, d\Omega + \oint_{d\Omega} [F - F_v]\, dS = 0 \tag{1}$$

where W means the conservative variables vector. F and F_v stand for convective flux vector and viscous flux vector, respectively.

$$W = [\rho \quad \rho u \quad \rho v \quad \rho E \quad \rho y_v \quad \rho y_g]^T \tag{2}$$

$$F = [\rho U \quad \rho u U + n_x p \quad \rho v U + n_y p \quad \rho U H \quad \rho y_v U \quad \rho y_g U]^T \tag{3}$$

U is a contravariant velocity that is normal to the surface element dS. y_v and y_g stand for the mass fractions of vapor and non-condensable gas phase, respectively.

2.2 System preconditioning

At low speed flow, system stiffness resulting from disparate convective and acoustic velocities causes deterioration of convergence rates. Convergence rates can be made independent of the Mach number by altering the acoustic speed of the system such that all eigenvalues are of the same order and thus the condition number approaches unity. We precondition the governing equations (Eq. (1)) by pre-multiplying the time derivative term by the preconditioning matrix from Weiss and Smith [7] as follows

$$\Gamma \frac{\partial}{\partial \tau} \int_{\Omega} Q \, d\Omega + \oint_{d\Omega} [F - F_v] \, dS = 0 \tag{4}$$

Where Q stands for the primitive variable vector given by

$$Q = [p \quad u \quad v \quad T \quad y_v \quad y_g]^T \tag{5}$$

and the preconditioning matrix Γ is

$$\boldsymbol{\Gamma} = \begin{bmatrix} \frac{1}{\beta} & 0 & 0 & \frac{\partial \rho}{\partial T} & \frac{\partial \rho}{\partial y_v} & \frac{\partial \rho}{\partial y_g} \\ \frac{u}{\beta} & \rho & 0 & \frac{\partial \rho}{\partial T} u & \frac{\partial \rho}{\partial y_v} u & \frac{\partial \rho}{\partial y_g} u \\ \frac{v}{\beta} & 0 & \rho & \frac{\partial \rho}{\partial T} v & \frac{\partial \rho}{\partial y_v} v & \frac{\partial \rho}{\partial y_g} v \\ H^* & \rho u & \rho v & \frac{\partial \rho}{\partial T} H + \rho \frac{\partial h}{\partial T} & \frac{\partial \rho}{\partial y_v} H + \rho \frac{\partial h}{\partial y_v} & \frac{\partial \rho}{\partial y_g} H + \rho \frac{\partial h}{\partial y_g} \\ \frac{y_v}{\beta} & 0 & 0 & \frac{\partial \rho}{\partial T} y_v & \frac{\partial \rho}{\partial y_v} y_v + \rho & \frac{\partial \rho}{\partial y_g} y_v \\ \frac{y_g}{\beta} & 0 & 0 & \frac{\partial \rho}{\partial T} y_g & \frac{\partial \rho}{\partial y_v} y_g & \frac{\partial \rho}{\partial y_g} y_g + \rho \end{bmatrix} \tag{6}$$

where

$$H^* = \frac{H}{\beta} + \rho \frac{\partial h}{\partial p} - 1 \tag{7}$$

The eigenvalues of the preconditioned system in equation (6) are given by

$$\lambda \left(\Gamma^{-1} \frac{\partial F}{\partial Q} \right) = U, U, U, U, U' - D, U' + D \tag{8}$$

where

$$U' = \frac{1}{2} \left(1 + \frac{c'^2}{c^2} \right) U \tag{9}$$

$$D = \frac{1}{2}\sqrt{\left(1 - \frac{c'^2}{c^2}\right)^2 U^2 + 4c'^2} \tag{10}$$

c is original speed of sound, and c' is preconditioned speed of sound given by

$$c' = \min(c, \max(\sqrt{u^2 + v^2}, V_{cutoff})) \tag{11}$$

In equation (11), V_{cutoff} is a cut-off value that is typically used to prevent the local velocity from becoming zero in the vicinity of stagnation region. The cut-off parameter V_{cutoff} is generally specified as $V_{cutoff} = kV_{\infty}$, where V_{∞} is a freestream velocity. In supersonic regime, the preconditioned speed of sound becomes the original speed of sound c, which means that preconditioning is turned off. Equation (4) is restricted to steady-state computations with pseudo-time τ. For unsteady computations, the dual-time stepping method is employed in which a preconditioned pseudo-time derivative term is introduced in addition to the physical time derivative in equation (1).

$$\Gamma \frac{\partial}{\partial \tau}\int_{\Omega} Q\, d\Omega + \frac{\partial}{\partial t}\int_{\Omega} W\, d\Omega + \oint_{d\Omega} [F - F_v]\, dS = 0 \tag{12}$$

where t denotes physical time and τ is pseudo-time used in the sub-iteration procedure. To obtain preconditioned speed of sound for unsteady computation, we use a preconditioning idea proposed by Venkateswaran and Merkle[4] that takes the effect of the Strouhal number into account through Von Neumann stability analysis of the dual-time stepping method. The resulting unsteady preconditioning parameter is given by

$$V = \frac{L}{\pi \Delta t} = \frac{L}{\pi \Delta t V} \times V = Str \times V \tag{13}$$

where L is a characteristic length scale and Δt is a physical time step size. The characteristic length scale is obtained as the problem domain size. Considering equation (13), the preconditioned speed of sound c' for unsteady flow is given by

$$c'_{un} = \min(c, \max(\sqrt{u^2 + v^2}, V_{cutoff}, V_{unsteady})) \tag{14}$$

For a large time step, V_{cutoff} is larger than $V_{unsteady}$, and then the preconditioned speed of sound is the same as in equation (11). For a small time step (that is, high Strouhal number), however, $V_{unsteady}$ is larger than local velocity magnitude $\sqrt{u^2 + v^2}$, so the unsteady preconditioning takes effect.

2.3 Scaling of numerical fluxes

For unsteady flow, evaluation of equation (9) and (10) by using steady preconditioned speed of sound results in excessive numerical dissipation related to the pressure difference term. The numerical dissipation related to the velocity difference term can be optimally scaled by using steady preconditioned speed of sound. For this reason, the scaling of dissipation terms should be carried out independently.

We apply the scaling function of AUSM+-up scheme[2] to the pressure dissipation term as follows:

$$\phi_p = \theta_p(2 - \theta_p) \tag{15}$$

where

$$\theta_p = \min(1, \max(\frac{\sqrt{u_{1/2}^2 + v_{1/2}^2}}{c_{1/2}}, \frac{V_{cutoff}}{c_{1/2}}, \frac{V_{unsteady}}{c_{1/2}})) \tag{16}$$

The subscript 1/2 means cell-interface value. As shown in equation (15), the unsteady preconditioned speed of sound is used to scale the pressure difference dissipation term. For velocity difference dissipation terms, the scaling based on local velocity is considered as follows:

$$\phi_v = \theta_v(2 - \theta_v) \tag{17}$$

where

$$\theta_v = \min(1, \max(\frac{\sqrt{u_{1/2}^2 + v_{1/2}^2}}{c_{1/2}}, \frac{V_{cutoff}}{c_{1/2}})) \tag{18}$$

3. CFD SIMULATIONS OF UNSTEADY CAVITATING FLOW AROUND A WEDGE

3.1 Problem description

The 2-D wedge used in this study has the wedge angle of 20 degrees and the depth of 20 millimeters. Table 1 shows the flow conditions and grid information, and figure 2 shows the grid system and boundary conditions. In this Table, σ_∞ stands for a cavitation number obtained by typical cavitation number formula. Another cavitation number σ, however, can be obtained by a formula considering blockage effect[9]. Because the computational domain is wall-bounded, the cavitation number σ is used in this study. Reynolds number and cavitation number are based on the freestream conditions and the wedge depth. The experiment in this study was carried out at the water tunnel of Chungnam National University. The tunnel has 100 by 100 millimeters test section, and its maximum freestream speed is 20m/s.

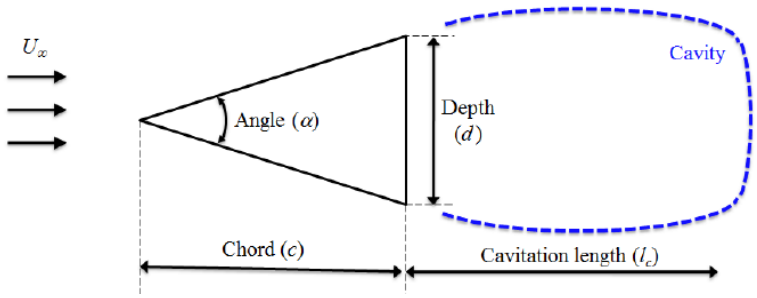

Figure 1. Schematic view of the problem

Table 1. Flow conditions and grid size

V(m/s)	P [kPa]	Re	σ_∞ (for infinite domain)	σ (for bounded domain)	Grid size
8.01	71,850	1.6×10^5	2.19	2.01	About 68,000 cells
8.05	58,300	1.6×10^5	1.75	1.52	
8.06	50,000	1.6×10^5	1.49	1.22	

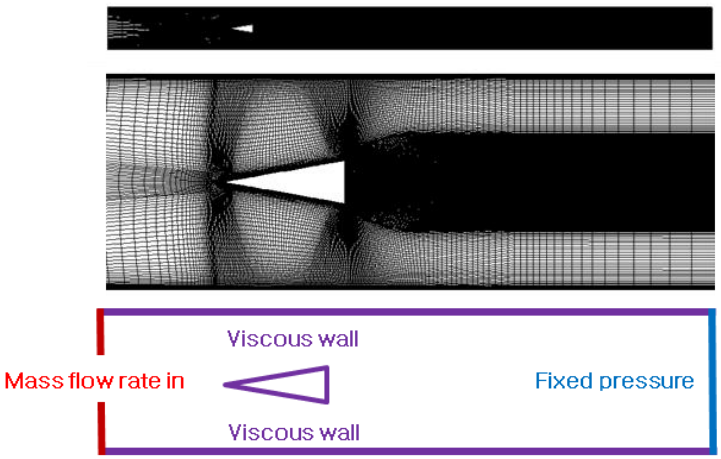

Figure 2. Grid system and boundary conditions

3.2 Results

The experimental results show that there are two types of shedding vortex as shown in figure 3; one of them is free shedding vortex, and the other is bounded shedding vortex that has relatively lower dominant frequency than free-shedding vortex. CFD simulations were carried out at the cavitation number of 1.22, 1.52, and 2.01; however, inflow pressure after computation is different from the initial input pressure that is required to obtain the cavitation numbers mentioned above, so the resulting cavitation numbers are also slightly different from those of experiments. Because the computational time did not sufficiently advance to catch the low-frequency bounded shedding vortex, the computed results show the dominant frequencies of the free

shedding vortex only. Figure 5 shows FFT analyses of numerical and experimental results. These results show the similar dominant frequencies of the free shedding vortices. Because of these similar dominant frequencies, the pattern and location of each shedding vortices are also similar in both numerical and experimental results.

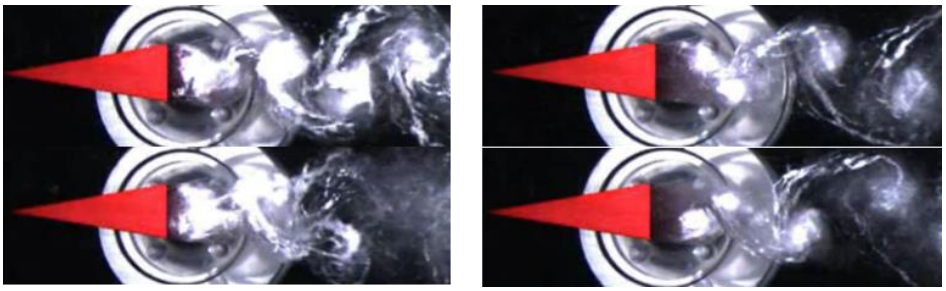

Figure 3. Two types of shedding vortex
(left: bounded shedding vortex, right: free shedding vortex)

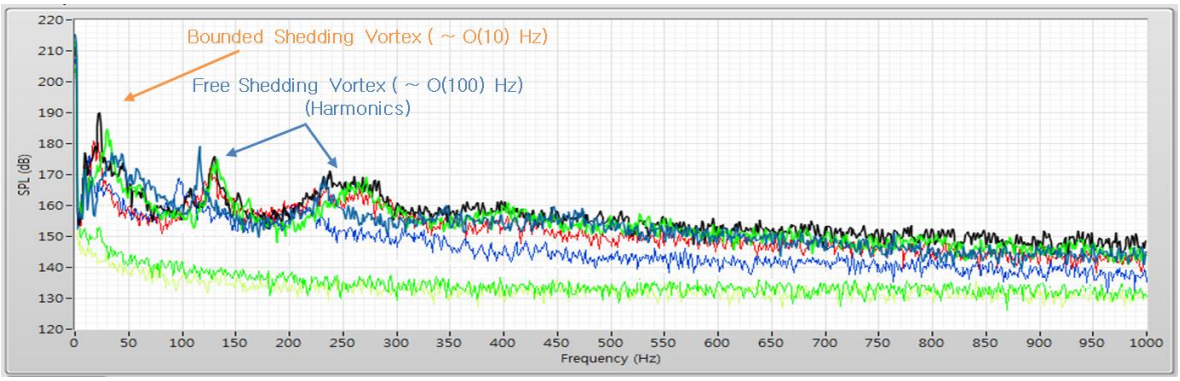

Figure 4. FFT analysis of the experimental results

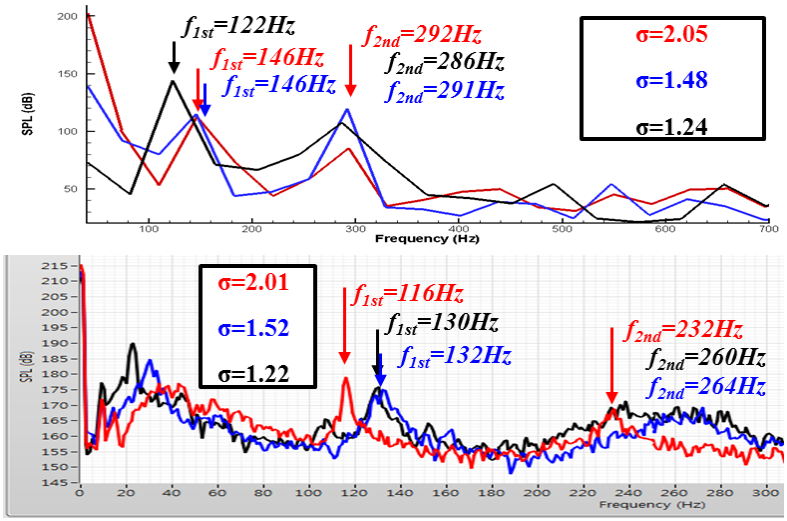

Figure 5. FFT analysis results (upper: CFD, lower: Exp.)

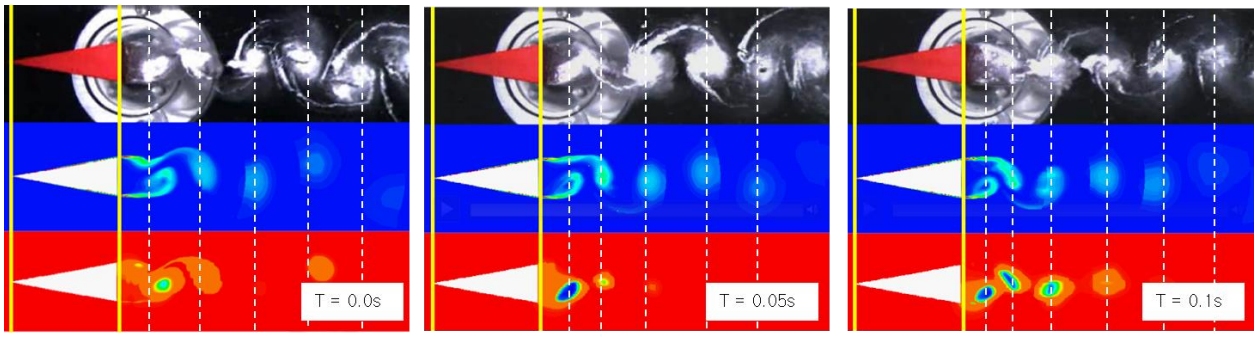

$\sigma = 1.22$ (in CFD, 1.24)

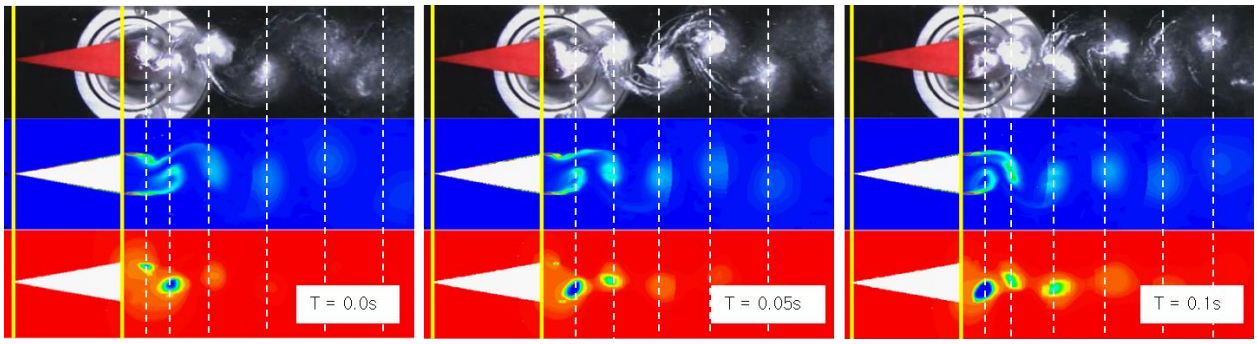

$\sigma = 1.52$ (in CFD, 1.48)

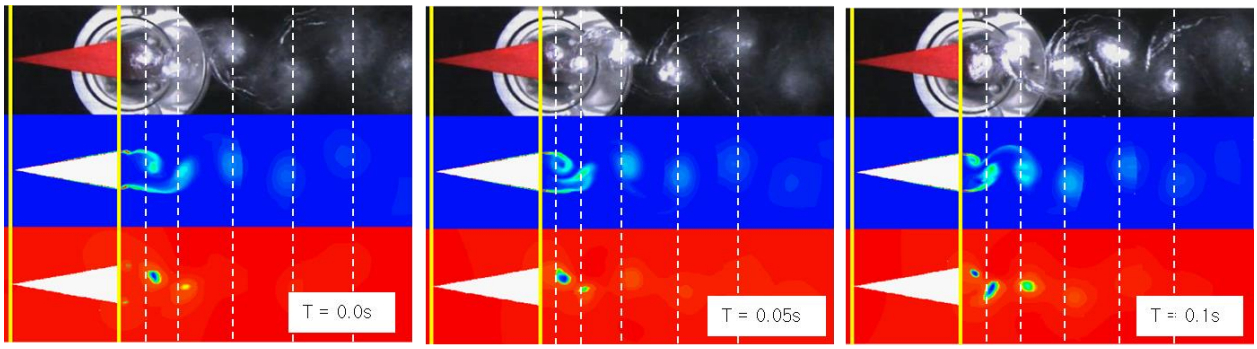

$\sigma = 2.01$ (in CFD, 2.05)

Figure 6. Snap shots of vortices at each specific time

4. CONCLUSIONS

URANS computations of cavitating flow around a 2-D wedge were carried out. For the accurate computation of unsteady low Mach number flow, we employed unsteady preconditioning technique to cluster system eigenvalues to similar order of magnitudes, and extended the previous all-speed two-phase RoeM and AUSMPW+ numerical flux schemes to the application of unsteady system preconditioning. We also scaled numerical dissipations of the RoeM and AUSMPW+ numerical flux schemes separately from the system preconditioning. With these solver and numerical methods, we

computed unsteady cavitating flow around a 2-D wedge model. The experimental results showed there were two types of shedding vortex; one of them was free shedding vortex, and the other was bounded shedding vortex that has relatively lower dominant frequency than free-shedding vortex. The computations and experiments showed similar results in terms of dominant frequencies of the free shedding vortex, pattern, and location of shedding vortices. Overall comparison confirmed that the present computations of unsteady cavitating flows show good agreement with the experimental results.

As a future work, we are planning to conduct more detailed numerical study to examine the behavior of the low-frequency bounded shedding vortex, and we are planning the extension to 3-D unsteady cavitating flow such as torpedoes with control fins.

ACKNOWLEDGMENTS

This research was supported by the program of Development of Space Core Technology (NRF-2015M1A3A3A05027630) and National Space Laboratory (NRF-2014M1A3A3A02034856) through the Ministry of Science, ICT & Future Planning. We also appreciate the financial supports provided by the Civil-Military Technology Cooperation Program.

REFERENCES

[1] J. M.Weiss, W. A. Smith, Preconditioning applied to variable and constant density flows, AIAA Journal 33 (11) (1995) 2050 - 2057.

[2] M.-S. Liou, A sequel to AUSM, Part II: AUSM+-up for all speeds, Journal of Computational Physics 214 (1) (2006) 137 - 170.

[3] X. song Li, C. wei Gu, Mechanism of Roe-type schemes for all-speed flows and its application, Computers & Fluids 86 (2013) 56 - 70.

[4] S. Venkateswaran, C. L. Merkle, Dual time-stepping and preconditioning for unsteady computations, in: 33rd Aerospace Sciences Meeting and Exhibit, Aerospace Sciences Meetings, American Institute of Aeronautics and Astronautics, Reno, Nevada, 1995.

[5] S.-W. Ihm, C. Kim, Computations of Homogeneous-Equilibrium Two-phase Flows with Accurate and Efficient Shock-Stable Schemes, AIAA Journal 46 (12) (2008) 3012 - 3037.

[6] S. Kim, C. Kim, O.-H. Rho, S. K. Hong, Cures for the shock instability: Development of a shock-stable Roe scheme, Journal of Computational Physics 185 (2) (2003) 342 - 374.

[7] K. H. Kim, C. Kim, O.-H. Rho, Methods for the Accurate Computations of Hypersonic Flows, Journal of Computational Physics 174 (1) (2001) 38 - 80.

[8] S. Venkateswaran, J. W. Lindau, R. F. Kunz, C. L. Merkle, Computation of Multiphase Mixture Flows with Compressibility Effects, Journal of Computational Physics 180 (1) (2002) 54 - 77.

[9] M.-S. Liou, C.-H. Chang, L. Nguyen, T. G. Theofanous, How to Solve Compressible Multi Fluid Equations: a Simple, Robust, and Accurate Method, AIAA Journal 46 (9) (2008) 2345 - 2356.

[10] J. Sachdev, A. Hosangadi, V. Sankaran, Improved Flux Formulations for Unsteady Low Mach Number Flows, in: 42nd AIAA Fluid Dynamics Conference and Exhibit, Fluid Dynamics and Co-located Conferences, American Institute of Aeronautics and Astronautics, New Orleans, Louisiana, 2012.

[11] A. J. Katz, D. Folkner, V. Sankaran, An Unsteady Preconditioning Scheme Based on Convective-Upwind Split-Pressure (CUSP) Artificial Dissipation, in: 52nd Aerospace Sciences Meeting, AIAA SciTech, American Institute of Aeronautics and Astronautics, National Harbor, Maryland, 2014.